

THE ANALYTICAL DESIGN OF A FOLDED WAVEGUIDE TRAVELING WAVE TUBE AND SMALL SIGNAL GAIN ANALYSIS USING MADEY'S THEOREM

F. Malek

Universiti Malaysia Perlis (UniMAP)
School of Computer and Communication Engineering
No. 12 & 14, Jalan Satu, Taman Seberang Jaya Fasa 3
Kuala Perlis 02000, Perlis, Malaysia

Abstract—We are developing an analytical model for the design of the folded waveguide traveling wave tube (FWTWT). This analytical model provides the physical view for rapid design optimization of the FWTWT. The design and analysis of the FWTWT using the spatial harmonics method of the TE_{10} mode of the EM wave are presented. An X-band FWTWT is used to verify this method. The normalized dispersion and beam line equations are used to simplify the design process so that the FWTWT can be designed to operate at any desired frequency. The small signal gain of an FWTWT is calculated by using Madey's theorem. The results of this analysis are compared with the numerical single particle simulation carried out using MATLAB. The results are in excellent agreement. The Madey's theorem can be used to provide a potential indication of the gain magnitude of the FWTWT.

1. INTRODUCTION

The first analysis of the folded waveguide traveling wave tube (FWTWT) was performed by Hutter in 1960. Dohler et al also did some work on an FWTWT at 45 GHz in the early 1990s [1, 2]. The FWTWT is an excellent candidate for many applications such as in communications, radar, military and medical fields, especially at millimeter-wave or terahertz frequencies [3–8]. The characteristics of the folded waveguide traveling wave tube fall under the umbrella of the general traveling wave tube (TWT) [9]. However, the present interest in the FWTWT is due to the work of Bhattacharjee, who has

Corresponding author: F. Malek (mfareq@unimap.edu.my).

shown that it is possible to combine vacuum electronics technology and silicon fabrication techniques to build miniature FWTWT, having sufficiently small broad and narrow dimensions that operation at very high frequencies would be possible [10,11]. When acting as sources, FWTWTs are predicted to be capable of producing milliwatts of output at terahertz frequencies with a low voltage (around 10 kV) and a low current (about 1 mA). Park and his co-workers have also been building low frequency prototype FWTWTs [12].

In this paper, we are developing an analytical model for the design of the folded waveguide travelling wave tube (FWTWT). Bhattacharjee has performed the simulation for the gain of FWTWT using state of the art TWT softwares [3]. However, the softwares do not provide the physical view for the rapid design optimization of the FWTWT. Han has performed the analytical study of the FWTWT, using the spatial harmonic method, but he did not provide a method to provide the optimum interaction between the electron beam and the EM wave dispersion curve [7]. In our approach, we firstly performed the spatial harmonic analysis to determine the beam-wave interaction for the FWTWT. In order to optimize the beam-wave interaction, the normalization method is used, so that all FWTWT designs would have identical beam-wave interaction dispersion curve plot. Different designs will only differ in the value of relative electron velocity, if the accelerating voltage of the beam is specified.

In the next step, the gain analysis of the FWTWT would be performed using Madey's theorem, where the electron-electron interaction would be neglected. Madey's theorem analysis of the FWTWT is important in order to study the small signal gain region of the FWTWT. In the future work, the gain of the FWTWT would be analyzed using the Pierce's theorem, where the space charge effects (electron-electron interaction) would be taken into consideration. Han appears to perform the gain analysis of the FWTWT using Pierce's theorem, and therefore the results of his study would only be applicable for the large signal gain region [7].

Glover has performed the gain analysis of the free electron laser (FEL) using Madey's theorem, where the wiggler wavelength, λ_w , of the FEL is included in the gain expression [13]. Therefore, our approach in this paper will provide the following benefits:

- (a) The normalization method of the spatial harmonic method would provide the correct beam-wave intersection, in order to obtain the optimum gain value for the FWTWT. Hence, appropriate dimensions of the FWTWT can be easily obtained to operate at any desired frequency, without resorting to numerical methods (softwares), at least not initially.

- (b) Glover has performed the small signal gain analysis on the free electron lasers [13]. Therefore, there is a need to perform the small signal gain analysis of the FWTWT using Madey's theorem. This would accurately predict the small signal gain of the FWTWT compared to the Pierce's theorem adopted by Han [7].
- (c) The small signal gain analysis of the FWTWT using Madey's theorem would then be verified by comparing the results with the results obtained from the numerical single particle analysis.

All TWTs have common operational structures. In a TWT, an electron gun, emitting an electron beam, is accelerated by the applied voltage into the interaction region. In this interaction region, energy exchange will occur between the traveling electrons and the EM wave. The electrons transfer energies to the EM waves, which results in the electrons being decelerated, before being dumped into the collector structure. The 'seed' electromagnetic wave in the interaction region will be amplified and can be extracted with the use of an appropriate coupler. The type of coupler usually depends on the frequency of operation of the TWT. A TWT can either operate in the oscillator mode or in the amplifier mode, where in the former case, an appropriate positive feedback is applied.

In the ensuing paragraphs, the operation of FWTWT is described in more detail. FWTWT uses an electric field plane (E -plane) bend rectangular waveguide, as can be seen in Figure 1 [3]. Circular apertures are drilled on the axial direction of the FWTWT. An electron in the beam crosses from the centre of one aperture to the centre of the next aperture in the straight line axial direction. The EM wave travels

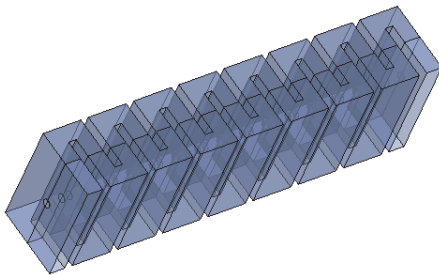


Figure 1. 3-D view of the folded waveguide traveling wave tube.

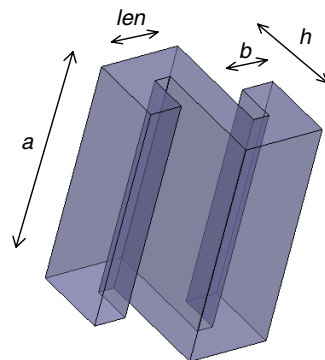


Figure 2. 3-D view of 1 period FWTWT indicating the dimension parameters.

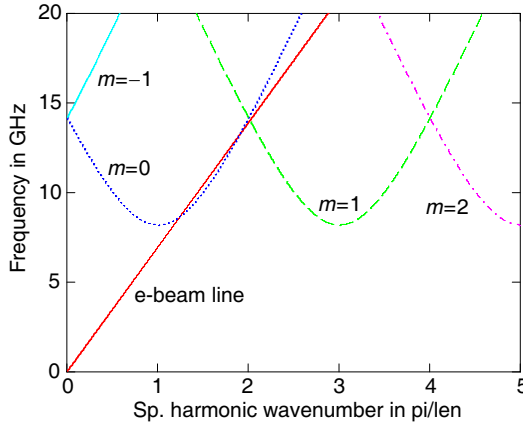


Figure 3. The dispersion curve for an FWTWT, with the beam line of electrons. The spatial harmonic numbers, m , associated with each branch are shown.

round the bend through the waveguide, as illustrated in Figures 2 and 3.

As an electron in the beam crosses one of the waveguide sections, it experiences either an accelerating or a decelerating force due to the transverse electric field of the TE_{10} mode of the EM wave propagating along the waveguide [14]. The height of the gap is designed such that each electron travels in the gap in less than half a period of the EM wave. A small amount of energy can be exchanged between an electron and the EM wave. When this electron reaches the next gap, it can find itself in the same phase relative to the electromagnetic wave provided the distance travelled by the faster wave is adjusted properly relative to the distance travelled by the electron. In this way, energy can be repeatedly and cumulatively transferred between the electrons and the EM wave in a similar way to a standard traveling wave tube (TWT) [4, 15–17].

As the accelerated electrons catch up with the decelerated electrons, bunching of electron occurs. The acceleration voltage can be adjusted accordingly so that more electrons will lose energy to the EM wave [4]. As a result the EM wave can be greatly amplified.

For effective coupling or energy exchange to occur, the electron and EM wave need to be traveling at the same velocity in order for the interaction to be cumulative. The phase velocity of the wave in FWTWT is slowed down to the velocity of an electron beam by its periodic structure [18]. In general periodic structures such as the disk loaded waveguide, stub loaded transmission line, the helical structure

and the coupled-cavity structure have periodic reactive load that can reduce the velocity of the EM wave traveling across the path [18, 19]. In FWTWT, the periodicity of the folded waveguide itself slows down the velocity of the EM wave.

If the velocity of the electron and the phase velocity of the EM wave are the same, the interaction is in synchronism. The synchronism requirement occurs at a particular frequency and phase constant, where the electron beam line and the EM wave dispersion curve intersects. This intersection can be shown in a ω - β plot.

To meet the synchronism requirement, the EM wave must be perturbed in some way. An EM wave traveling within an empty straight waveguide would have the phase velocity always greater than or equal to the speed of light. Therefore, it is impossible to accelerate an electron beam to meet the synchronism requirement because relativity provides an upper limit of 'c' on the speed of the electron beam. By perturbing the EM wave within the waveguide, the EM wave axial phase velocity is reduced. As a result, in FWTWT, the EM wave axial phase velocity is smaller than the velocity of light in vacuum. Therefore, FWTWT is also known as the slow wave structure.

2. THE DESIGN OF FWTWT

The FWTWT design parameters consist of the physical dimensions of the waveguide cross section (a and b), the len and h dimensions, as well as the electron beam acceleration potential, v_{acc} , in order for the FWTWT to operate in a certain frequency. The maximum gain is expected to happen if the FWTWT parameters are designed correctly.

The dispersion relationship and the electron beam characteristics are functions of these design parameters and allow a design equation to be derived [20–25]. An appropriate normalization procedure allows the normalized design equation to be derived. The normalized design equation consists of normalized parameters, and allows all parameters to be determined if any one of them is known.

In the FWTWT system, strong interactions can only take place at frequencies near to the dispersion curve and the electron beam line intersections. It is easier to analyze the operations of FWTWT in terms of spatial harmonics of the TE₁₀ mode [26].

The m -th spatial harmonics is given by [7]

$$\omega^2 = \omega_{co}^2 + \left(\frac{c \cdot len}{len + h} \right)^2 \left[k - (2m + 1) \frac{\pi}{len} \right]^2 \quad (1)$$

where len and h are the dimensions of the FWTWT, as can be seen in Figure 2. The angular cut-off frequency, ω_{co} is given by $\frac{c\pi}{a}$ where a

is the broad dimension of the waveguide and c is the speed of light in vacuum. k is the wavenumber of the spatial harmonic and is not the same as the wavenumber of the TE_{10} mode, k_g , which travels through a straight rectangular waveguide [27–29]. The dispersion curve equation of a straight rectangular waveguide is shown in (2)

$$\omega^2 = \omega_{co}^2 + c^2 k_g^2 \quad (2)$$

The electron beam line equation is given as follows:

$$\omega = v_e k \quad (3)$$

v_e is the average velocity of the electrons in the beam.

An example dispersion curve for a FWTWT having $a = 18.36$ mm, $b = 2.701$ mm, $len = 4.051$ mm and $h = 8.931$ mm is shown in Figure 3. The electron beam line is accelerated at 9.25 kVolts. The spatial harmonic numbers, m , associated with each branch are shown. Notice that the horizontal axis is plotted in units of $\frac{\pi}{len}$ so that the minimum of the $m = 0$ branch happens at $k = \pi/len$.

To obtain an effective interaction in FWTWT, the electron beam should be synchronized with the $m = 0$ spatial harmonic of the EM wave. The $m = 0$ spatial harmonic is chosen as the operating point, as it has the largest spatial harmonics amplitude among the entire spatial harmonic components. For the case of forward wave FWTWT, to obtain a reasonable bandwidth, the dispersion curve line of the EM wave in the ω - β plot should be tangential to the e-beam line. Without an appropriate analytical method, it is difficult to design an optimum FWTWT, as there are many design parameters involved, such as ' a ', ' len ', ' b ', ' h ' and ' v_{acc} '.

For dispersion curves, it is very convenient to plot the normalized angular frequency versus the normalized wavenumber [26, 30]. In order to simplify the design process, the normalized dispersion curve for the $m = 0$ spatial harmonic is given as follows [26]:

$$\left(\frac{\omega}{\omega_{co}}\right)^2 = 1 + \left(\frac{len}{len + h}\right)^2 \left(\frac{k}{k_{co}} - \frac{a}{len}\right)^2 \quad (4)$$

where $k_{co} = \frac{\omega}{c} = \frac{\pi}{a}$ is the cut-off wavenumber of the spatial harmonic.

By using the normalization procedure, Equation (4) can be written as

$$y^2 = 1 + r^2(x - s)^2 \quad (5)$$

where

$$\begin{aligned} y &= \frac{\omega}{\omega_{co}} & x &= \frac{k}{k_{co}} \\ r &= \frac{len}{len + h} & s &= \frac{a}{len} \end{aligned} \quad (6)$$

Similarly, the normalized beam line equation can be written as

$$\frac{\omega}{\omega_{co}} = \frac{v_e k}{c \cdot k_{co}} \quad \text{or} \quad y = \beta_e x \quad (7)$$

β_e is the average velocity of an electron in the beam relative to the velocity of light. Equations (5) and (7) can be solved simultaneously to find the intersection points of the dispersion curve with the electron beam line.

For the forward EM wave case, the electron beam line is tangential to the dispersion curve to give broadband operation. This means, the point of tangential contact between the electron beam line and the dispersion curve is at the point $k_{op} = \frac{3\pi}{2 \cdot len}$ which is half way between the cut-off wavenumber, $k = \frac{\pi}{len}$ and the point where the $m = 0$ spatial harmonics intersects with the $m = 1$ spatial harmonic (at $k = \frac{2\pi}{len}$).

For the backward EM wave case, the electron beam line intersects with the EM dispersion curve at $k = \frac{\pi}{2 \cdot len}$, which is between the point of intersection at $m = -1$ spatial harmonic and $m = 0$ spatial harmonic and the cut-off wavenumber. In this paper the analysis of backward wave FWTWT is performed.

With this choice of operating point for the backward wave EM case, hence x_{op} can be shown to be as follows.

$$x_{op} = \frac{k_{op}}{k_{co}} = \frac{\pi}{2 \cdot len} \frac{a}{h} = \frac{a}{2 \cdot len} = \frac{s}{2} \quad (8)$$

By substituting this value of x_{op} in Equation (8) into Equation (4), and substituting Equation (3) into Equation (4), the following expression can be obtained:

$$\beta_e^2 = \left(\frac{2}{s}\right)^2 + r^2 \quad (9)$$

It is reasonable to assume that the frequency of operation is $1.5 * f_{co}$. By using this assumption, we then obtain the following expression.

$$1.25c^2 \frac{\pi^2}{a^2} = \left(\frac{c \cdot len}{len + h}\right)^2 \left(\frac{\pi}{2len}\right)^2 \quad (10)$$

Equation (10) can be simply written as follows.

$$r^2 = \frac{5}{s^2} \quad (11)$$

By substituting Equation (11) into Equation (9), the expression for β_e can be obtained.

$$\beta_e = \frac{3}{s} \quad (12)$$

Therefore different backward wave FWTWT designs will differ only in the value of the relative electron velocity, β_e . This will then determine the factor, s , if the accelerating voltage, V_{acc} is known.

By substituting Equations (8) and (12) into Equation (9), we obtained the following expression:

$$y_{op} = 1.5 \quad (13)$$

Hence, for $m = 0$ spatial harmonic, the normalized dispersion Equation (5) and the beam line Equation (7) can be derived.

$$y = \sqrt{1 + 5 \left[\left(\frac{x}{s} \right) - 1 \right]^2} \quad \text{and} \quad y = 3 \left(\frac{x}{s} \right) \quad (14)$$

As a result, if Equation (14) are plotted with the vertical axis as y , and the horizontal axis as $(\frac{x}{s})$, hence all possible backward wave FWTWT have identical graphs as shown in Figure 4. The solid curve is the $m = 0$ spatial harmonic, while the dotted line is the e-beam line.

As can be seen in Equation (13), the normalized frequency of operation, y_{op} is independent of s . Hence, y_{op} is independent of the acceleration voltage, V_{acc} for any design. This allows the broad dimension of the waveguide for any particular frequency to be determined immediately as follows:

$$f_{op} = \frac{1.25c}{a} \quad (15)$$

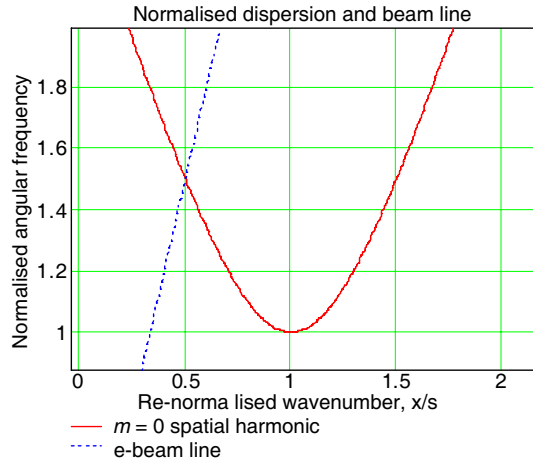


Figure 4. Normalized dispersion and beam line for backward wave FWTWT.

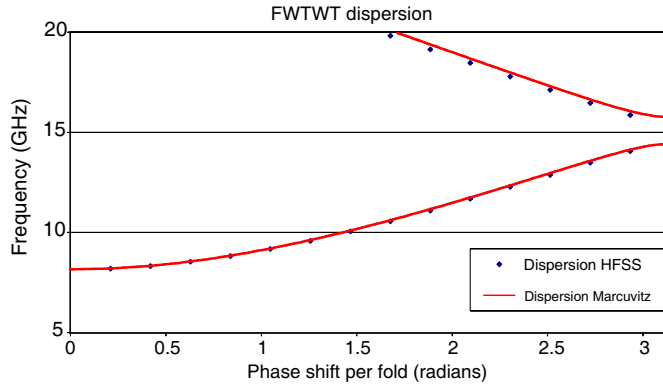


Figure 5. The FWTWT dispersion curve comparison between the numerical simulation (using Ansoft HFSS) and the marcuvitz theorem equivalent circuit model.

In the next step, a particular value of the acceleration voltage, V_{acc} is chosen. The relative electron velocity, β_e can be obtained as follows:

$$\beta_e = \sqrt{1 - \left(\frac{511}{511 + V_{acc}} \right)^2} \quad (16)$$

If β_e is now known, hence, the value s can be determined from Equation (12). Since s is also defined as $\frac{a}{len}$ as in Equation (6), the value of len can now be determined. Finally, by using Equations (6) and (11), the value h can be determined.

To determine the value of the narrow dimension of the waveguide, b , we can assume that the transit time of electron across the narrow dimension of the waveguide, $\frac{b}{v_e}$ is equal to one-fifth period of the EM wave, $\frac{1}{5f_{op}}$. Hence, b , can be determined if the frequency of operation, f_{op} and the accelerating voltage, V_{acc} , are known. b is given as follows:

$$b = \frac{\beta_e c}{5f_{op}} \quad (17)$$

The equivalent circuit model for the waveguide can make the design process easier [31–33]. The Marcuvitz theorem is used to determine the equivalent circuit model of sharp corners for the FWTWT [32]. The dispersion curve of a 15-fold FWTWT is simulated using Ansoft HFSS software. Figure 5 illustrates the result of this HFSS simulation, which is compared with the result obtained using Marcuvitz method. The solid line indicates the dispersion curve obtained using the equivalent

circuit method, while the dotted points indicate the dispersion curve using HFSS simulation. As can be seen in Figure 5, there is a very close agreement between the simulation results using HFSS and the equivalent circuit model which uses the Marcuvitz theorem. This shows that the equivalent circuit model can be used to derive the dispersion curve of the FWTWT.

3. EXAMPLE DESIGN OF AN FWTWT

To verify our method, an example design of FWTWT is performed in the X-band spectrum. A backward wave FWTWT is to be constructed to operate at 10 GHz with a 10 kV electron beam. Therefore a is given by

$$a = \frac{1.25c}{f_{op}} = 37.47 \text{ mm}$$

With an accelerating voltage of 10 kV, β_e equals to 0.195. Hence, len can be derived as follows:

$$s = \frac{3}{\beta_e} = 15.38$$

$$len = \frac{a}{s} = 2.36 \text{ mm}$$

The value of h is then given by

$$h = len \left\{ \frac{s}{\sqrt{5}} - 1 \right\} = 13.87 \text{ mm}$$

The narrow dimension of the FWTWT structure is given by

$$b = \frac{\beta_e c}{5f_{op}} = 1.17 \text{ mm}$$

A check is made to ensure that $len - b > 0$. This condition is met in this design, and hence, the design is valid. If this had not been so, an alternative, lower accelerating voltage would have had to be chosen and the dimensions recalculated.

4. GAIN OF FWTWT USING MADEY'S THEOREM

Bhattacharjee has performed simulations on the design of FWTWT sources for Terahertz radiation, using state of the art TWT softwares [3]. However, the softwares do not provide the physical insight for rapid design optimization of the FWTWT. Han has performed analysis and simulations for the design of FWTWT taking space charge effects into account, i.e., the electron-electron interactions

are considered, using the Pierce's theorem [7]. Pierce theorem combines the Eulerian view of the electron beam with the replacement of the delay line as propagation structure by an equivalent transmission line model consisting of distributed inductances, L and capacitances, C [16, 34].

However, Park has not studied the effect of the gain of the FWTWT using Madey's theorem. The FWTWT design analysis using Madey's theorem is important in order to arrive at the optimum operation of the FWTWT in the small signal gain region. In this small signal gain region, the effect of space charge between the electrons are not taken into the design consideration. The FWTWT device operating in the small signal gain region (low acceleration voltage and current) could be useful to avoid effects that might reduce the stability of the output. Glover has analyzed the gain of a free electron laser using Madey's theorem [13]. The gain analysis of the free electron laser using Madey's theorem is related to the parameter wiggler wavelength, λ_w , and therefore is could not be applied to FWTWT.

So far, we have analyzed the FWTWT in terms of spatial harmonics of the TE_{10} mode propagation of the EM wave. By using the normalization method, the dimension parameters of the FWTWT could be obtained if the frequency of operation and the acceleration voltage are specified. In this section, the small signal gain of an FWTWT is calculated by using the Madey's theorem.

Figure 6 shows the plan view of the FWTWT, showing the dimension parameters used. A TE_{10} mode propagation of the wave is assumed to be traveling in the $+z'$ direction, as shown in Figure 5 [35, 36]. An electron beam is passed through the FWTWT from left to right, in the $+z$ direction, as shown in Figure 6. The interaction between the electron beam and the EM wave in the waveguide can be thought of in terms of the electrons with a fictitious continuous slow wave that propagates along the z -axis [37].

Hutter's original analysis of the dispersion relationship of an FWTWT states that an expansion into spatial harmonics is possible using the following equation [1]:

$$\vec{e}(z, t) = \hat{z} \cdot \text{Re} \left\{ \sum_{m=-\infty}^{\infty} A_E \frac{b}{len} \text{sinc} \left(\frac{k_m^+ b}{2} \right) \exp[j(\omega t - k_m^+ z)] \right\} \quad (18)$$

Equation (18) is the field in the gaps of the FWTWT. k_m^+ represents a spatial harmonic with positive group velocity. Hence, this running wave is carrying power in the positive z -direction, and is a forward wave along the same direction as the electron beam. A_E is the amplitude of the E -field of the TE_{10} mode propagation of the wave in the waveguide having frequency, ω , and the FWTWT wavenumber, k_g .

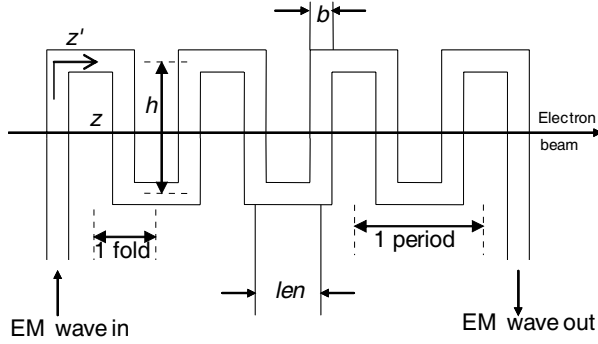


Figure 6. A plan view of an FWTWT, showing the dimensions. ‘ b ’ is the narrow dimension of the waveguide, while ‘ a ’ is the wide dimension of the rectangular waveguide (into the paper).

The expression of the general spatial harmonic wavenumbers, k , is given by

$$k = k_m^\pm = \left\{ (2m + 1) \frac{\pi}{len} \pm k_g \left(\frac{len + h}{len} \right) \right\} \quad (19)$$

where m is an integer ranging from $-\infty$ to $+\infty$. The expression for k_g is as follows.

$$k_g = \frac{1}{c} \sqrt{\omega^2 - \omega_{co}^2} \quad (20)$$

In the FWTWT, the electron beam will interact with these spatial harmonics. In amplifier configuration, it is possible to achieve synchronism with only one spatial harmonic at a time. For the FWTWT operation, the $m = 0$ forward wave spatial harmonic is considered, since this results in a higher harmonic amplitude [31, 32]. This then leads to a greater interaction and hence higher gain. The $m = 0$ forward spatial harmonic is represented as an EM wave in the $+z$ direction by the electric field, shown as follows [13, 38].

$$\vec{e}_0^+ = \frac{A_E b}{len} \text{sinc} \left(\frac{k_0^+ b}{2} \right) \cos(\omega t - k_0^+ z) \hat{z} \quad (21)$$

where

$$k = k_0^+ = \frac{\pi}{len} + k_g \left(\frac{len + h}{len} \right) \quad (22)$$

The field contribution can be used with Madey’s theorem to calculate the gain of the FWTWT. This z -directed field effects the energy of

electrons in such a way that

$$\frac{d}{dt}(\gamma mc^2) = -e \cdot \vec{e}_0^+ \cdot \vec{v} \quad (23)$$

The left hand side of Equation (23) represents the rate of increase of the energy of an electron, while the right hand side is the rate at which work is done on the electron by the electric field. The right hand side of Equation (23) is approximated by assuming that the electron velocity is hardly changed by the interaction. Hence,

$$\vec{v} = \vec{v}_0 = v_{z0} \hat{z} \quad (24)$$

where v_{z0} is the unperturbed electron velocity. This means that the amplitude A_E , of the EM wave is also hardly affected, so it may be taken as a constant. Equation (23) can be written as follows.

$$\frac{d\gamma}{dt} = -\frac{e}{mc^2} A_E \frac{b}{len} v_{z0} \text{sinc}\left(\frac{k_0^+ b}{2}\right) \cos(\omega t - k_0^+ z + \varphi) \quad (25)$$

where a phase, φ , has been introduced to allow for a range of entry times of an electron into the FWTWT. The expression $\omega t - k_0^+ z = z[\frac{\omega}{v_{z0}} - k_0^+]$ can be written, where $\nabla k = \frac{\omega}{v_{z0}} - k_0^+$.

By dividing both sides of Equation (25) by v_{z0} , and using $dz = v_{z0} dt$, the following expression is obtained.

$$\frac{d\gamma}{dz} = -F \cdot \cos(\omega t - k_0^+ z + \varphi) = -F \cdot \cos(\nabla k \cdot z + \varphi) \quad (26)$$

where

$$F = \frac{e}{mc^2} A \frac{b}{len} \text{sinc}\left(\frac{k_0^+ b}{2}\right) \quad (27)$$

Both sides of Equation (26) are integrated from $z = 0$ to $z = N \cdot len$, where N is the number of folds in the FWTWT. By using the trigonometric identity $2 \sin(A) \cos(B) = \sin(A + B) + \sin(A - B)$, the overall change, γ_1 , in relative energy from entrance to exit is given as follows.

$$\begin{aligned} \gamma_1 &= \int_0^{Nlen} -\frac{F}{\nabla k} \sin(\nabla k \cdot z + \varphi) dz \\ &= \frac{-2F}{\nabla k} \sin\left(\frac{\nabla k \cdot N \cdot len}{2}\right) \cos\left(\frac{\nabla k \cdot N \cdot len}{2} + \varphi\right) \end{aligned} \quad (28)$$

If the electron entry times are distributed uniformly in phase from $-\pi$ to $+\pi$, then Equation (28) indicates that as many electrons will gain energy as will lose energy. Therefore, no net exchange of energy between the electrons and the EM wave occurs. This is expressed by

stating that the average energy change per electron is zero, or, $\llbracket \gamma_1 \rrbracket = 0$, where $\llbracket \dots \rrbracket$ indicates averaging over phase, φ .

Several approximations have been made in deriving Equation (28). Hence, this is only a first order result. If better approximations are made it is found that there is a small but finite change in total energy of the electrons, so that for the second order result, $\llbracket \gamma_2 \rrbracket \neq 0$.

In Madey's theorem, the second order energy change $\llbracket \gamma_2 \rrbracket$ can be related to the previously calculated, first order energy change, $\llbracket \gamma_1 \rrbracket$ [13]. Madey's theorem states that

$$\llbracket \gamma_2 \rrbracket = \frac{1}{2} \frac{d}{d\gamma} \llbracket \gamma_1^2 \rrbracket \quad (29)$$

If the average of the square of γ_1 is determined, therefore $\llbracket \gamma_1 \rrbracket$ can be solved directly by performing the required differentiation.

Squaring Equation (26) gives

$$\gamma_1^2 = \left(\frac{2F}{\nabla k} \right)^2 \sin^2 \left(\frac{\nabla k \cdot N \cdot len}{2} \right) \cdot \cos^2 \left(\frac{\nabla k \cdot N \cdot len}{2} + \varphi \right) \quad (30)$$

Averaging on φ gives

$$\gamma_1^2 = \frac{1}{2} \left(\frac{2F}{\nabla k} \right)^2 \sin^2 \left(\frac{\nabla k \cdot N \cdot len}{2} \right) \quad (31)$$

Substituting Equation (31) into the Second Order Madey's theorem, and using $x = \frac{\nabla k \cdot N \cdot len}{2}$, the following expression is obtained.

$$\begin{aligned} \llbracket \gamma_2 \rrbracket &= \frac{1}{4} (F \cdot N \cdot len)^2 \frac{d}{dx} \text{sinc}^2 \left(\frac{\nabla k \cdot N \cdot len}{2} \right) \Big|_{x=\frac{\nabla k \cdot N \cdot len}{2}} \\ &\quad \frac{d}{d\gamma} \left(\frac{\nabla k \cdot N \cdot len}{2} \right) \end{aligned} \quad (32)$$

Since $\text{sinc}(x) = \frac{\sin(x)}{x}$, the following expression is obtained.

$$\begin{aligned} \frac{d}{dr} \left(\frac{\nabla k \cdot N \cdot len}{2} \right) &= \frac{N \cdot len}{2} \frac{d}{d\gamma} \left(\frac{\omega}{V_{z0}} - k_0^+ \right) = \frac{N \cdot len \cdot \omega}{2} \frac{d}{d\gamma} \left(\frac{1}{v_{z0}} \right) \\ &= \frac{-N \cdot len \cdot \omega}{2 \cdot v_{z0}^2} \frac{dv_{z0}}{d\gamma} = \frac{-N \cdot len \cdot \omega}{2 \cdot c \cdot \beta_{z0}^3 \gamma^3} \end{aligned} \quad (33)$$

where $\beta_{z0} = \frac{v_{z0}}{c}$ is the relative electron velocity, and γ is the relativistic mass factor of an electron. Therefore, the average energy gained per electron in passing through N folds of the FWTWT is given by.

$$\llbracket \gamma_2 \rrbracket mc^2 = \frac{-1}{4} (F \cdot N \cdot len)^2 \frac{d}{dx} \text{sinc}^2 \left(\frac{\nabla k \cdot N \cdot len}{2} \right) \frac{N \cdot len \cdot \omega}{2 \cdot c \cdot \beta_{z0}^3 \gamma^3} mc^2 \quad (34)$$

If the electron beam current is I_e , then $\frac{I_e}{e}$ electrons pass into the FWTWT per second. Hence, the total power lost by the electrons and therefore the power gained by the EM wave is

$$P_{out} - P_{in} = \llbracket \gamma_2 \rrbracket mc^2 \frac{I_e}{e} = \frac{1}{4} (F \cdot N \cdot len)^2 \frac{d}{dx} \text{sinc}^2 \left(\frac{\nabla k \cdot N \cdot len}{2} \right) \frac{N \cdot len \cdot \omega \cdot m \cdot c^2 I_e}{2c\beta_{z0}^3 \gamma^3 e} \quad (35)$$

where $x = \frac{\nabla k \cdot N \cdot len}{2}$. P_{in} is the EM wave power entering the FWTWT and P_{out} is the power leaving the FWTWT. The gain of the FWTWT is defined as the ratio of the increase in power gained by the EM wave to the input EM wave power, i.e., $\frac{P_{out} - P_{in}}{P_{in}}$. The FWTWT gain is different from the electronic gain, which is the ratio of output power to the input power, $\frac{P_{out}}{P_{in}}$. For the TE₁₀ mode of the wave propagation in a rectangular waveguide, the input power is given by [39]

$$P_{in} = \frac{1A_E^2 a \cdot b \cdot c \cdot k_g}{4.120\pi \cdot \omega} \quad (36)$$

Therefore, the FWTWT gain is given by

$$\text{Gain}_{\text{FWTWT}} = \frac{\left(\frac{e \cdot N \cdot b}{2 \cdot m \cdot c^2} \right)^2 \text{sinc}^2 \left(\frac{k_0^+ b}{2} \right) \cdot \left(\frac{N \cdot len \cdot \omega}{2 \cdot \beta_{z0}^3 \gamma^3 c} \right) \cdot \left(\frac{m \cdot c^2}{e} \right) \cdot I_e \cdot \frac{d}{dx} \text{sinc}^2(x)}{\left(\frac{1 \cdot a \cdot b \cdot c \cdot k_g}{4.120\pi \cdot \omega} \right)} \quad (37)$$

Where the differential coefficient is evaluated at $x = \frac{\nabla k \cdot N \cdot len}{2}$. It can be shown that the FWTWT gain is proportional to N^3 . A MATHCAD program is designed to view the result of the gain plot of FWTWT using Madey's theorem. The general parameters used in this MATHCAD program is shown in Table 1.

Figure 7 shows the FWTWT gain plot using Madey's theorem. The x -axis is the frequency sweep from 8.5 to 12 GHz, while the y -axis is the FWTWT gain values. The largest gain occurs at 9.735 GHz at with a gain of 0.8817, or 88.17%. The gain of the FWTWT in Equation (37) seems to be independent of frequency for a fixed electron gun current and accelerating voltage and a fixed number of folds. However, if the operating frequency is increased, the dimensions of the FWTWT have to be decreased in proportion. Hence, the dimensions of the hole through which the electron beam travels are also reduced. Therefore, the electron beam current would also have to be reduced as the operating frequency is increased. This reduction is required so that we do not lose too much beam current by interception to the walls of the FWTWT.

Table 1. The general parameters used to determine the gain of FWTWT using Madey’s theorem.

| | |
|-----------------|---------------|
| V_{acc} | 8.70 kV |
| N | 40 |
| Frequency sweep | 8.5 to 12 GHz |
| I_e | 5 mA |
| A | 18.359 mm |
| B | 2.701 mm |
| Len | 4.051 mm |
| H | 8.931 mm |

Table 2. The FWTWT dimensions used so that the results can be compared with Bhattacharjee’s work [3].

| | |
|-------|-------------------|
| a | 300 μm |
| b | 43 μm |
| len | 66 μm |
| h | 70 μm |

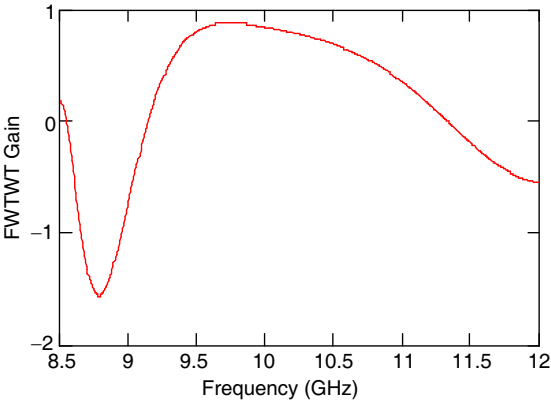


Figure 7. The plot of the gain of FWTWT using Madey’s theorem.

The results obtained using the small signal gain analysis using Madey’s theorem would now be compared with the work done by Bhattacharjee [3]. The FWTWT designed by Bhattacharjee operates at the frequency of 560 GHz. For this comparison exercise, the FWTWT dimensions used as input parameters into Equation (3) are shown in Table 2.

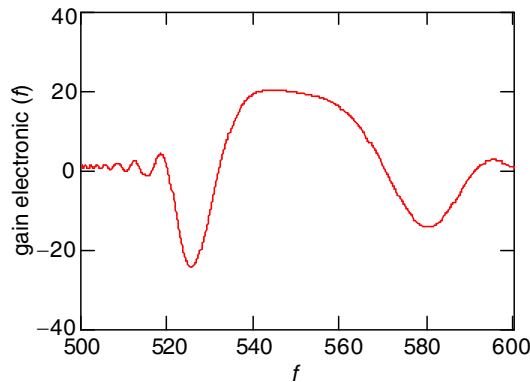


Figure 8. Electronic gain versus frequency for FWTWT.

The dimensions quoted in Table 2 are not all the same as quoted by Bhattacharjee, since he used semicircular folds in his design, not the sharp bends analyzed in our design [3]. For this comparison purpose, our FWTWT device was assumed to be driven with an electron beam with an acceleration voltage of 10.64 kV and a current of 0.5 mA. Bhattacharjee quotes 10.9 kV and 0.5 mA [3]. The FWTWT device as an input parameter into Equation (37) has 220 number of folds, N . The calculations from Equation (37) show that the maximum electronic gain is 20.26, or equivalent to 13.1 dB. This occurs at 543.9 GHz, and is shown in Figure 8.

Bhattacharjee's simulations were performed with the state of the art TWT softwares (MAFIA, TW3 and CHRISTINE), and gave an electronic gain of about 13 dB at a frequency of 542 GHz [3]. However, Bhattacharjee's device consisted of just 100 folds compared with the 220 used in our simulation [3]. Since the power gained by the EM wave is proportional to N^3 , as shown in Equation (35), therefore the agreement appears much better than it actually is. Based on Bhattacharjee's simulation, the gain of FWTWT is much greater than is predicted by our Equation (35).

The approach adopted in our paper, using Madey's theorem is a small signal gain model, i.e., the model can only accurately predict small signal gains. As can be seen in Figure 11, the derived maximum gain is very large, i.e., the output power could not be stated as only marginally larger than the input.

5. GAIN OF FWTWT USING NUMERICAL SINGLE PARTICLE SIMULATION

The gain of the FWTWT is now being calculated using the numerical single particle simulation [13]. In this simulation, the equations of motion of an electron passing through the FWTWT are solved [13]. The results obtained using these simulations are compared with the analytical method using Madey's theorem.

From Equation (25), the equation that governs the motion of electrons is given by the following expression.

$$\frac{d\gamma}{dt} = -\frac{e}{mc^2} A_E \frac{b}{len} v_z(t) \text{sinc}\left(\frac{k_0^+ b}{2}\right) \cos(\omega t - k_0^+ z + \varphi) \quad (38)$$

Using, Newton's Force Law, $\frac{d}{dt}(\gamma m_0 v) = -e \cdot E$, the following expressions are obtained.

$$\frac{d[\gamma(t) m v_z(t)]}{dt} = -e A_E \frac{b}{len} \text{sinc}\left(\frac{k_0^+ b}{2}\right) \cos(\omega t - k_0^+ z + \varphi) \quad (39)$$

$$\frac{dz(t)}{dt} = v_z(t) \quad (40)$$

Equations (38)–(40) can be written in terms of dz by using the relationship $dt = \frac{dz}{v_z(t)}$.

$$\frac{d\gamma(z)}{dz} = -\frac{e}{mc^2} A_E \frac{b}{len} \text{sinc}\left(\frac{k_0^+ b}{2}\right) \cos(\omega t - k_0^+ z + \varphi) \quad (41)$$

Using Newton's Force Law, $\frac{d}{dt}(\gamma m_0 v) = -e \cdot E$, we obtained the expression $\frac{dv_z(z)}{dt} = \frac{-e \cdot E}{m \cdot \gamma^3}$. By substituting $dt = \frac{dz}{v_z(t)}$ into $\frac{dv_z(z)}{dt} = \frac{-e \cdot E}{m \cdot \gamma^3}$, we obtain the following expressions.

$$\frac{dv_z(z)}{dz} = -\frac{e}{\gamma^3 m v_z(z)} A_E \frac{b}{len} \text{sinc}\left(\frac{k_0^+ b}{2}\right) \cos(\omega t - k_0^+ z + \varphi) \quad (42)$$

$$\frac{dt(z)}{dz} = \frac{1}{v_z(z)} \quad (43)$$

Equations (41)–(43) are solved using MATLAB program, utilizing the Ordinary Differential Equation (ODE) built-in function. A set of electrons, uniformly distributed in phase from $-\pi$ to π , are simulated passing through the FWTWT. The electrons' final energies, $\gamma \cdot N \cdot len \cdot m \cdot c^2$ are averaged. Any reduction in energy for the electron means an increment of energy of the EM wave. Hence, the gain of the FWTWT using numerical single particle simulation can be obtained. The general parameters used in the MATLAB program are shown in Table 3.

Table 3. The general parameters used in the MATLAB program to determine the gain of FWTWT using numerical single particle analysis simulation.

| | |
|-----------|-----------|
| V_{acc} | 8.70 kV |
| N | 40 or 3 |
| I | 5 mA |
| f | 9.735 GHz |
| a | 18.359 mm |
| b | 2.701 mm |
| h | 8.931 mm |
| len | 4.051 mm |
| P_{in} | 50 mW |

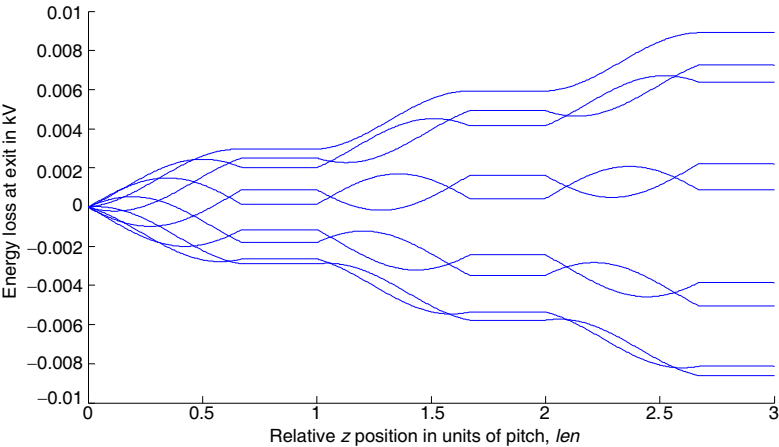


Figure 9. The variation of electron energy loss with position down the FWTWT. $N = 3$, $I = 5$ mA and 9 electrons are used. The electrons are uniformly distributed in phase from $-\pi$ to $+\pi$.

The variations of the energy of electrons as they travel down the axis of an FWTWT are plotted in Figures 9 to 12. The first plot, Figure 9, shows the results using $N = 3$ folds, $I = 5$ mA and 9 number of electrons. The second plot, Figure 10, shows the results using $N = 3$ folds, $I = 5$ mA and 5 number of electrons. The third plot, Figure 11, shows the results using $N = 40$ folds, $I = 5$ mA and 9 number of electrons. The fourth plot, Figure 12, shows the results using $N = 40$ folds, $I = 5$ mA and 5 number of electrons.

The x -axis is the relative z position in units of z/len , while the y -axis indicates the energy loss at exit in kV. The different curves in Figures 9–12 indicate the energy loss (in kV) of the electrons (with different phases) as they travel down the FWTWT along the z -axis.

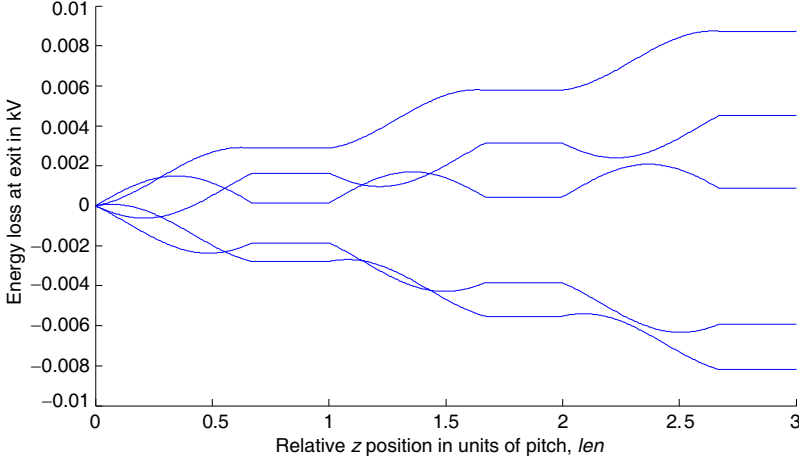


Figure 10. The variation of electron energy loss with position down the FWTWT. $N = 3$, $I = 5$ mA and 5 electrons are used. The electrons are uniformly distributed in phase from $-\pi$ to $+\pi$.

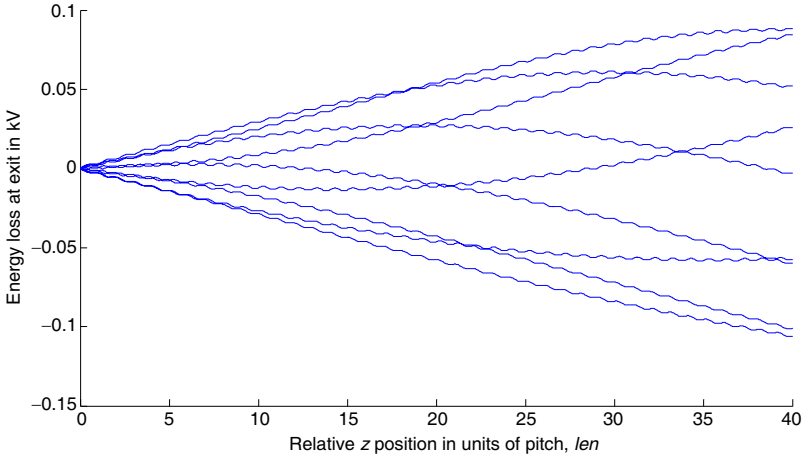


Figure 11. The variation of electron energy loss with position down the FWTWT. $N = 40$, $I = 5$ mA and 9 electrons are used. The electrons are uniformly distributed in phase from $-\pi$ to $+\pi$.

Each electron is interacting with a spatially discontinuous electric field that only exists in the waveguide gaps of the FWTWT. On average, an electron takes one and a half cycles of the EM wave to cross the gap. The curves are obtained for FWTWT having gaps which are one and a half cycles of the EM wave. This effect can be seen more clearly in Figures 9 and 10, where the number of folds, N , is made equal to 3. As an example, taking the lowest curves in Figures 9 and 10, there are no energy changes for the distance traveled in the first two half cycles. Only the last half cycle contributes. In between the gaps, the energy remains constant.

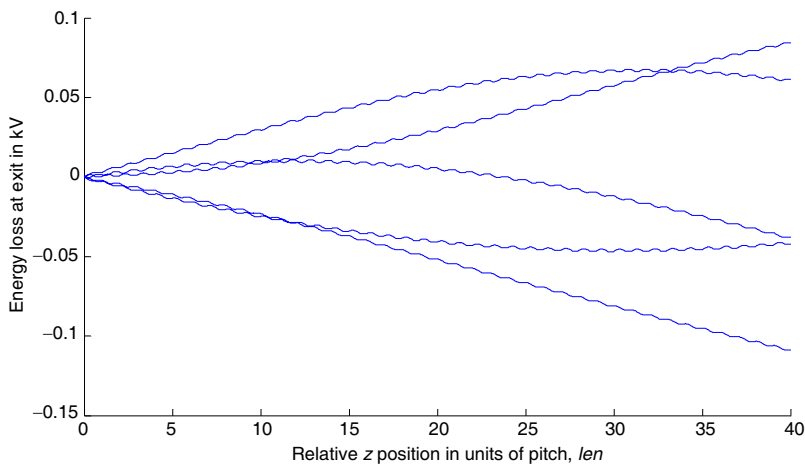


Figure 12. The variation of electron energy loss with position down the FWTWT. $N = 40$, $I = 5\text{ mA}$ and 5 electrons are used. The electrons are uniformly distributed in phase from $-\pi$ to $+\pi$.

Table 4. Comparison of the gain of FWTWT using Madey’s theorem and numerical analysis.

| | Madey’s Theorem | Numerical Single Particle Analysis |
|--|-------------------------|------------------------------------|
| $I = 5\text{ mA}$; $N = 40$, 9 number of electrons used for numerical single particle analysis | FWTWT Gain = 88.02% | FWTWT Gain = 85.33% |
| $I = 8\text{ mA}$; $N = 40$, 9 number of electrons used for numerical single particle analysis | FWTWT Gain = 140.83% | FWTWT Gain = 136.53% |

The gain results for the Madey's theorem and the numerical analysis are included in Table 4. The agreement between the numerical analysis and the Madey's theorem is excellent in spite of the fact that only 9 electrons are used. It is expected that the agreement between the two methods can be improved if larger number of electrons are used. However, the run time of the MATLAB program using larger number of electrons will be longer.

6. CONCLUSION AND FUTURE WORK

In this paper, we have succeeded in deriving an analytical model for the design of an FWTWT to operate at any desired frequency, with examples given for the backward wave FWTWT case. Using the spatial harmonic method analysis and the normalization procedure, with the knowledge of the operating frequency, f_{op} and acceleration voltage, V_{acc} , the user can therefore obtain the dimension parameters of any desired FWTWT. The analysis we proposed in this paper ensures that intersection point between electron beam line and the dispersion curve occurs at the desired point for optimum beam-wave interaction. For forward wave FWTWT, this occurs at the half way point between the cut-off frequency of $m = 0$ spatial harmonic and the intersection point between $m = 0$ and $m = 1$ spatial harmonics. For backward wave FWTWT, this occurs at the half way point between the cut-off frequency of $m = 0$ spatial harmonic and the intersection point between $m = -1$ and $m = 0$ spatial harmonics.

The gain of an FWTWT in the small gain, single electron regime has been investigated. The small gain model using Madey's theorem has been adopted. Madey's theorem can accurately predict small gains. An analytical formula derived by using the Madey's theorem has been developed. The numerical simulation of the electron beams interacting with the EM wave has also been performed. The results of the analysis using Madey's theorem have been confirmed numerically by the single particle analysis simulation.

For the Madey's theorem to be applicable, the amplitude A_E , of the EM wave remains unchanged by the interaction with the electron beams. The Madey's theorem applied for FWTWT covers the initial, small signal gain region, which means for short length and low current FWTWT. Therefore, the number of folds and the general parameters chosen (as shown in Tables 1 and 3) for the Madey's theorem and numerical single particle simulation are small so that small gain conditions apply. Hence, in practice, the Madey's theorem model can be used provided that the FWTWT gain is limited to less than about 2.9. Although the Madey's theorem gain formula can only represent

a practical situation where the maximum FWTWT gain is less than about 2.9, the formula does provide a potential figure of any particular device that is useful in the initial stages of a design.

If larger number of folds and beam current are used, the results using Madey's theorem show that the FWTWT has a much greater gain than the magnetostatic and Cherenkov FELs. Therefore, Madey's theorem can be used to provide a potential indication of the gain magnitude of FWTWT. On the other hand, it is an advantage to operate an FWTWT oscillator in the small signal gain regime, where Madey's theorem applies in order to avoid problems with mode competition, mode hopping, and other effects that might reduce the stability of the output.

Madey's theorem is a single electron model, where the electron-electron interactions or space charge effects are ignored. Pierce's theory, which includes the space charge effects, states that after the EM wave has traveled a short distance through the device where its growth is low, the gain of the EM wave becomes exponential, which is significantly more than the N^3 dependence predicted by Madey's theorem [40]. In the future, further work will be performed to investigate the gain of the FWTWT using Pierce's theorem.

REFERENCES

1. Hutter, R. G. E. and S. W. Harrison, *Beam Wave Electronics in Microwave Tubes*, Princeton University Press, Princeton, New Jersey, 1960.
2. Dohler, G., D. Gallagher, and J. Richards, "Millimeter wave folded waveguide TWTs," *Vacuum. Electron. Ann. Rev. Proc.*, Vol. 15–20, 1993.
3. Bhattacharjee, S., J. H. Booske, C. L. Kory, D. W. Van Der Weide, S. Limbach, J. D. Welter, M. R. Lopez, R. M. Gilgenbach, R. L. Ives, M. E. Read, R. Divan, and D. C. Mancini, "Folded waveguide traveling-wave tube sources for terahertz radiation," *IEEE Transactions on Plasma Science*, Vol. 32, No. 3, 1002–1014, June 2004.
4. Stuart, R. A., A. I. Al-Shamma'a, and J. Lucas, "Compact tuneable terahertz source," *2nd EMRS DTC Technical Conference-Edinburgh*, 2005.
5. Singh, G., "Analytical study of the interaction structure of vane-loaded gyro-traveling wave tube amplifier," *Progress In Electromagnetics Research B*, Vol. 4, 41–66, 2008.
6. Booske, J. H., M. C. Converse, C. L. Kory, C. T. Chevalier,

- D. A. Gallagher, K. E. Kreischer, V. O. Heinen, and S. Bhattacharjee, "Accurate parametric modeling of folded waveguide circuits for millimeter-wave traveling wave tubes," *IEEE Transactions on Electron Devices*, Vol. 52, No. 5, 685–694, May 2005.
7. Han, S.-T., J.-I. Kim, and G.-S. Park, "Design of a folded waveguide traveling-wave tube," *Microwave and Optical Technology Letters*, Vol. 38, No. 2, 161–165, July 20, 2003.
 8. Yang, T., S. Song, H. Dong, and R. Ba, "Waveguide structures for generation of terahertz radiation by electro-optical process in GaAs and ZnGeP₂ using 1.55 μm fiber laser pulses," *Progress In Electromagnetics Research Letters*, Vol. 2, 95–102, 2008.
 9. Wang, W., Y. Wei, G. Yu, Y. Gong, M. Huang, and G. Zhao, "Review of the novel slow-wave structures for high-power traveling-wave tube," *International Journal of Infrared and Millimeter Waves*, Vol. 24, No. 9, 1469–1484, September 2003.
 10. Kory, C. L., J. H. Booske, W.-J. Lee, S. Gallagher, D. W. Van Der Weide, S. Limbach, and S. Bhattacharjee, "THz radiation using high power, microfabricated, wideband TWTs," *International Microwave Symposium Digest 2, IEEE MTT-S International*, 1265–1268, 2002.
 11. Bhattacharjee, S., J. H. Booske, C. L. Kory, D. W. Van Der Weide, S. Limbach, M. Lopez, R. M. Gilgenbach, and M. Genack, "THz radiation using compact folded waveguide TWT oscillators," *International Microwave Symposium Digest 2, IEEE MTT-S International*, 1331–1334, 2003.
 12. Park, G.-S., H.-J. Ha, W.-K. Han, S.-S. Jung, C.-W. Baik, and A. Ganguly, "Investigation of folded waveguide TWT," *25th International Conference on Infrared and Millimeter Waves*, 279–280, 2000.
 13. Glover, L. K. and R. H. Pantell, "Simplified analysis of free-electron lasers using Madey's theorem," *IEEE Journal of Quantum Electronics*, Vol. 21, No. 7, July 1985.
 14. Qin, P.-Y., C.-H. Liang, and B. Wu, "Novel dual-mode bandpass filter with transmission zeros using substrate integrated waveguide cavity," *Journal of Electromagnetic Waves and Applications*, Vol. 22, No. 5–6, 723–730, 2008.
 15. Gittins, J. F., *Power Travelling-wave Tubes*, The English Universities Press Ltd., 1964.
 16. Pierce, J. R., *Traveling-wave Tubes*, D. Van Nostrand Company, Inc., 1950.

17. Liu, S., "Study of propagating characteristics for folded waveguide TWT in millimeter wave," *International Journal of Infrared and Millimeter Waves*, Vol. 21, No. 4, 655–660, 2000.
18. Harvey, A. F., "Periodic and guiding structures at microwave frequencies," *IRE Trans. Microwave Theory Techn.*, Vol. 8, 30–61, 1960.
19. Collin, R. E., *Foundations for Microwave Engineering*, McGraw-Hill, New York, 1992.
20. Reutskiy, S. Y., "The methods of external excitation for analysis of arbitrarily-shaped hollow conducting waveguides," *Progress In Electromagnetics Research*, PIER 82, 203–226, 2008.
21. Psarros, I. and I. D. Chremmos, "Resonance splitting in two coupled circular closed-loop arrays and investigation of analogy to traveling-wave optical resonators" *Progress In Electromagnetics Research*, PIER 87, 197–214, 2008.
22. Hernandez-Lopez, M. A. and M. Quintillan-Gonzalez, "A finite element method code to analyse waveguide dispersion," *Journal of Electromagnetic Waves and Applications*, Vol. 21, No. 3, 397–408, 2007.
23. Sjöberg, D., "Determination of propagation constants and material data from waveguide measurements," *Progress In Electromagnetics Research B*, Vol. 12, 163–182, 2009.
24. Heh, D. Y. and E. L. Tan, "Dispersion analysis of FDTD schemes for doubly lossy media," *Progress In Electromagnetics Research B*, Vol. 17, 327–342, 2009.
25. Kalyanasundaram, N. and G. N. Babu, "Dispersion of electromagnetic waves guided by an open tape Helix I," *Progress In Electromagnetics Research B*, Vol. 16, 311–331, 2009.
26. Stuart, R. A., "The design of folded waveguide travelling wave tubes," A report for FELDEC, October 16, 2004.
27. Nie, Z.-P., S. Yan, S. He, and J. Hu, "On the basis functions with traveling wave phase factor for efficient analysis of scattering from electrically large targets," *Progress In Electromagnetics Research*, PIER 85, 83–114, 2008.
28. Su, D. Y., D.-M. Fu, and Z.-H. Chen, "Numerical modeling of active devices characterized by measured S -parameters in FDTD," *Progress In Electromagnetics Research*, PIER 80, 381–392, 2008.
29. Vaish, A. and H. Parthasarathy, "Analysis of a rectangular waveguide using finite element method," *Progress In Electromagnetics Research C*, Vol. 2, 117–125, 2008.
30. Shahi, A. K., V. Singh, and S. P. Ojha, "Dispersion

- characteristics of electromagnetic waves in circularly cored highly birefringent waveguide having elliptical cladding,” *Progress In Electromagnetics Research*, PIER 75, 51–62, 2007.
31. Mondal, M. and A. Chakrabarty, “Resonant length calculation and radiation pattern synthesis of longitudinal slot antenna in rectangular waveguide,” *Progress In Electromagnetics Research Letters*, Vol. 3, 187–195, 2008.
 32. Marcuvitz, N., *Waveguide Handbook*, Peregrinus, Stevenage, U.K., 1986.
 33. Che, W., C. Li, D. Wang, L. Xu, and Y. Chow, “Investigation on the ohmic conductor losses in substrate-integrated waveguide and equivalent rectangular waveguide,” *Journal of Electromagnetic Waves and Applications*, Vol. 21, No. 6, 769–780, 2007.
 34. Eichmeier, J. A. and M. Thumm, *Vacuum Electronics: Components and Devices*, Springer, 2008.
 35. Carle, P. L., “New accurate and simple equivalent circuit for circular E -plane bends in rectangular waveguide,” *Electronics Letters*, Vol. 23, No. 10, 531–532, May 7, 1987.
 36. Panda, D. K. K., A. Chakrabarty, and S. R. Choudhury, “Analysis of Co-channel interference at waveguide joints using multiple cavity modeling technique,” *Progress In Electromagnetics Research Letters*, Vol. 4, 91–98, 2008.
 37. Sumathy, M., K. J. Vinoy, and S. K. Datta, “Equivalent circuit analysis of serpentine folded waveguide slow-wave structures for millimeter-wave traveling wave tubes,” *International Journal of Infrared and Millimeter Waves*, Vol. 30, No. 2, 151–158, February 2009.
 38. Stuart, R. A., “The gain of a FWTWT,” A report for FELDEC, November 12, 2004.
 39. Pozar, D. M., *Microwave Engineering*, John Wiley & Sons, Inc., 1998.
 40. Kumar, D., P. K. Choudhury, and O. N. Singh, “Towards the dispersion relations for dielectric optical fibers with helical windings under slow- and fast-wave considerations — A comparative analysis,” *Progress In Electromagnetics Research*, PIER 80, 409–420, 2008.